JOURNAL OF MATERIALS SCIENCE 29 (1994) 328–337

X-ray analysis of the structure of a thermotropic main-chain liquid-crystalline copolyester

E. M. ANTIPOV*, M. STAMM‡, E. W. FISCHER
Max-Planck-Institut für Polymerforschung, Postfach 3148, 55021 Mainz, Germany

The structure and phase behaviour of the thermotropic main-chain liquid-crystalline copolyester poly[(phenyl-*p*-phenylene)-co-(terephthalate)-co-(*p*-hydroxybenzoate)] (PES) prepared from terephthalic acid, phenylhydroquinon and *p*-hydrobenzoic acid (molar ration 45/45/10) is determined by X-ray diffraction and differential scanning calorimetry. This random copolyester shows up to 340 °C periodic *c*-axis order in its X-ray diffraction pattern as well as sharp and diffuse reflections at the equator and other crystallographic directions, indicating well ordered three-dimensional crystalline structure. Two crystalline modifications are observed for quenched and annealed fibres, which are both orthorhombic with slightly different unit cell sizes. Indications of other phases at still higher temperatures are reported. They are believed to be a novel mesophase followed by a nematic liquid-crystalline phase and the isotropic melt.

1. Introduction

During the last 10 years there has been an increasing interest in the development of wholly aromatic main chain thermotropic liquid-crystalline (LC) polyesters in both academic and industrial areas of research. From the engineering point of view, their low viscosity in the melt and the self-reinforcement due to the ability of LC polymers to orientate their rigid backbones during processing, make these materials one of the most promising classes for future applications in industry. From the scientific viewpoint, the attraction is based on the fact that it is possible in principle, as discussed in [1], that novel mesophases may exist in such polymeric systems besides the typical LC states already observed.

Although a number of studies on those materials have been reported [2–7], the nature of crystalline and mesophase structures of thermotropic LC copolyesters is still under discussion, and in particular the temperature behaviour is far from being understood. In order to gain further insight into the crystalline and mesophase structures and their transitions, we have studied fibres of a wholly aromatic copolyester (PES) using DSC and X-ray diffraction techniques at ambient and higher temperatures.

2. Experimental procedure

2.1. Materials and samples

The copolyester fibres, kindly provided by Prof. A.V. Volokhina (USSR), denoted in this paper PES-fibres, were prepared from 0.45 mole of terephthalic acid, 0.45 mole of phenylhydroquinone and 0.10 mole of *p*-hydroxybenzoic acid, and are believed to be random copolymers due to preparation conditions. The copolyester was synthesized via a direct condensation reaction of the three monomers in solution. To increase the molecular mass, solid-state polymerization was carried out after precipitation and drying of the copolyester at 260 °C for 10 h in vacuum.

Relative viscosities were measured in a mixture of acetic acid and chloroform (60/40%) at a concentration of 0.5 g per 100 ml. For samples with different times of chemical reaction they were equal to 3.4, 4.4 and 4.7, respectively.

The preparation of melt–spun fibres was carried out from the nematic phase (320 °C). The diameter of a single fibre amounts to about 1 μm. The fibres were examined (a) in the as-spun state and (b) after annealing in vacuum for 4 h at different temperatures with free ends, followed by quenching.

Specimens for X-ray analysis were prepared in parallel bundles with about 300 fibres. In order to perform differential scanning calorimetry (DSC), the fibre samples were put into DSC pans. Sample weights were typically in the range 10–20 mg.

2.2. Wide-angle (WAXS) and small-angle (SAXS) X-ray diffraction

X-ray experiments were carried out on an 18 kW Rigaku X-ray generator. A rotating Cu anode was

* Permanent address: Institute of Petrochemical Synthesis, Russian Academy of Sciences 117912, Moscow, Leninsky pr 29, Russia.
‡ Author to whom correspondence should be addressed.

0022–2461

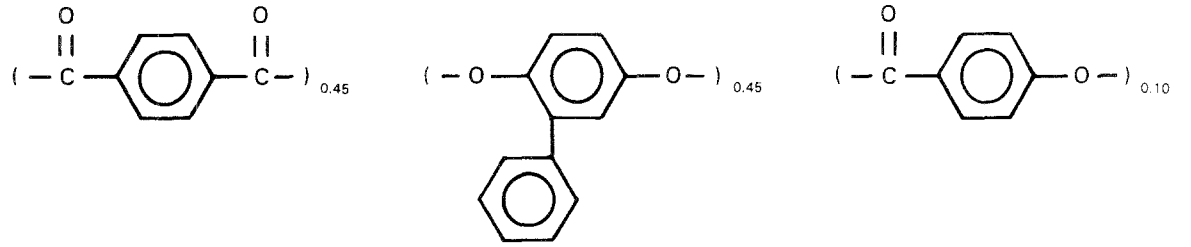

Scheme 1 Chemical composition of poly[(phenyl-*p*-phenylene)-co-(terephthalate)-co-(*p*-hydroxybenzoate)] (PES).

used as the source of the primary beam. The CuK_α beam, typically of 0.5 mm diameter, was monochromatized with two graphite crystals and registered by a curved area gas detector with energy discrimination. X-ray fibre patterns were recorded in transmission geometry with the sample mounted in a vacuum chamber provided with a (heatable) sample holder. The versatile geometry of the equipment allowed the use of WAXS or SAXS regimes by a change of the detector position. The maximal total length of the setup is 3 m, and a typical exposure time is 10 h.

Equatorial and meridional X-ray diagrams were recorded in reflection geometry on a standard Siemens X-ray θ–θ diffractometer D500T equipped with scintillation counter. The slit-focused beam was monochromatized with a graphite crystal. In addition a pulse-height analyser sensitive to CuK_α radiation was used. Temperature measurements were carried out under vacuum in a heatable sample holder. The wavelength in both diffractometers is 0.154 nm.

2.3. Differential scanning calorimetry (DSC)

A Mettler TA 4000 was used to determine the temperature behaviour and transition temperatures of the samples. The fibres were heated from room temperature to 380 °C at a heating rate of 20 °C min^{-1} and held there for 10 min. They then were subsequently cooled at the same rate to room temperature and some samples then heated again. In order to avoid the influence of previous thermal treatment every sample was used only once.

3. Results and discussion

Before presenting structural studies, the phase behaviour of samples with different thermal histories will be described.

3.1. Calorimetric measurements

Fig. 1 shows the DSC traces of the as-spun fibres of PES copolymers with different relative viscosities. These curves have a complicated character and reveal several thermal events. They have several features in common. During the first heating runs weak broad endothermal effects between 150 °C and 270 °C and two relatively strong endo-maxima at ~ 300 °C and 320 °C are observed. Perhaps another very weak endo-peak is located at ~ 350–360 °C. Besides endo-maxima, one can suspect the existence of at least one exothermal feature at 270 °C.

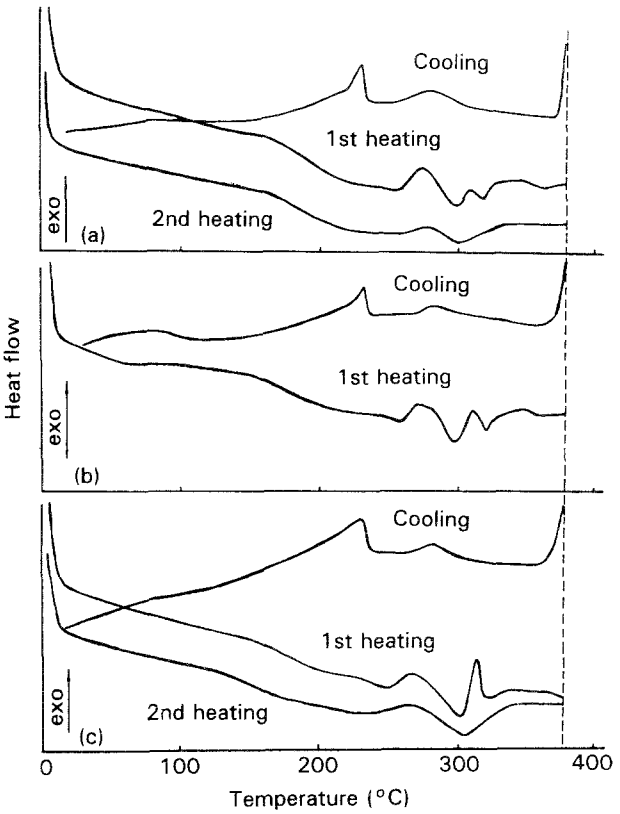

Figure 1 DSC traces for PES fibres with relative viscosities: 3.4 (a); 4.4 (b); 4.7 (c). (Heating/cooling rate 20 °C min^{-1})

In cooling, strong and weak exo-maxima are observed in DSC traces located at 230 °C and 280 °C, respectively. The second heating runs show the same behaviour as the first, but have a more smeared character due to the broadening of endo- and exo-peaks. Since all of the three samples exhibit in principle the same behaviour during heating and cooling, results concerning only the fibre with viscosity 4.4 will be discussed in detail below.

Fig. 2 shows the DSC traces of the as-spun and quenched, as well as of the annealed, fibres. It is obvious that the curves for the annealed sample exhibit a quite different behaviour from the ones for the as-spun fibre during first heating. In the latter case we observe two well-pronounced endo-maxima, shifted to higher temperatures as compared to the unannealed sample. The cooling and second heating traces are almost the same as for the as-spun sample.

In order to understand the nature of these heating phenomena, a series of annealing treatments were carried out. Fibres with non-fixed (free) ends were heated in glass capillaries to 150, 180, 210, 240, 270, 300, 310, 320, 330, 340, 350 and 360 °C under vacuum.

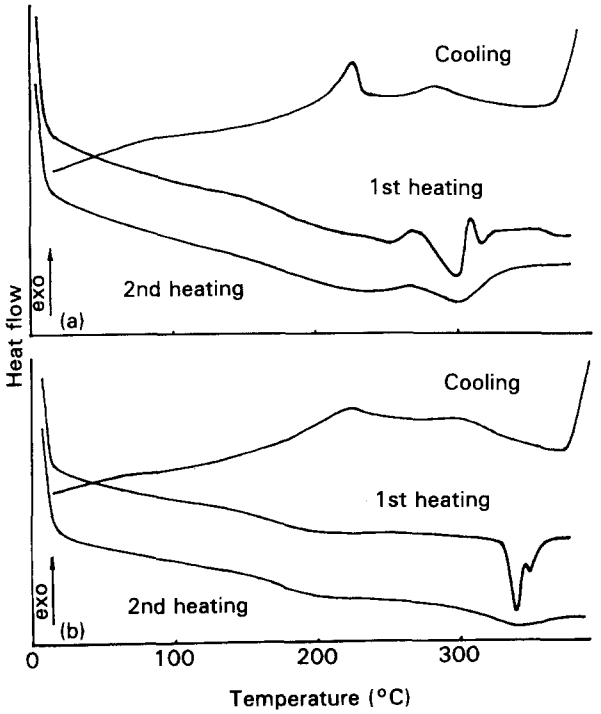

Figure 2 DSC traces for PES fibres (relative viscosity 4.4) quenched (a) and annealed (b) for 1 h at 290 °C, 9 h at 300 °C and 6.5 h at 320 °C.

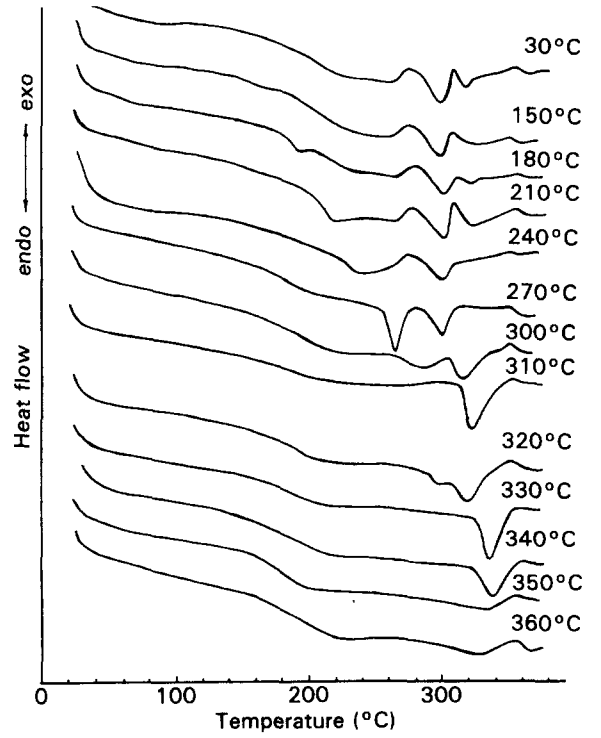

Figure 3 DSC traces during heating (1st run) for PES fibres previously annealed for 4 h with free ends at the indicated temperatures.

After holding the temperature for 4 h, each sample was quenched to 25 °C.

DSC measurements for those annealed samples are presented in Fig. 3. At annealing temperatures below 270 °C the well-known effect [8] of the appearance of a maximum corresponding to the temperature of annealing is observed. Otherwise the character of the DSC curves is generally the same as for the as-spun fibre. After annealing at 270 °C the DSC diagram shows two well-pronounced endo-maxima at 270 °C and 300 °C and a weak endo-peak at ~ 360 °C. This can be taken as an indication that at least three differential structural forms are possible for PES fibres. Treatment at still higher temperatures shows that only one strong maximum at 320–340 °C now remains in the DSC picture. Thus the low temperature structural form seems to disappear when the annealing temperature is equal or larger than 310 °C. At 350 °C and higher temperatures a common broadening of the DSC curves is observed.

In conclusion, several important thermal regions are identified from DSC investigations of PES fibres, namely $T < 270$ °C, $T = 270$–340 °C and $T > 340$ °C. They should be also reflected in a careful X-ray analysis.

Fig. 4 shows a typical WAXS fibre diagram from the area detector for the quenched PES copolyester. Different intensity levels are indicated by different colours, ranging from black (low intensity) through blue, green, red, yellow and white (high intensity) on a non-linear scale. The dark spot in the middle corresponds to the beam stop, and an angular range of approx. − 35° to + 35° is shown. Equatorial and meridional diffraction scans registered for the same sample on the θ–θ goniometer are shown in Fig. 5.

The X-ray pattern shown in Fig. 4 exhibits a strong diffuse scattering in the equator over an angular range of approximately 10–35°, and two other weaker spots at $2\theta \sim 5$–$9°$ and ~ 12–16° (see Fig. 5a). Three narrow and very strong Bragg reflections are presented in the meridian at 14.25, 28.72 and 43.67° (see Fig. 5b), which correspond to different orders of a reflection in the 2nd, 4th and 6th layer lines, indicating a $P2_1$ space group. The scattered intensity of odd orders is very weak, but still detectable in the diffraction curve with strong amplification (Fig. 5c).

From the character of the X-ray patterns one might suggest that the quenched PES fibre is at least a two phase system. For the first phase one can suspect that

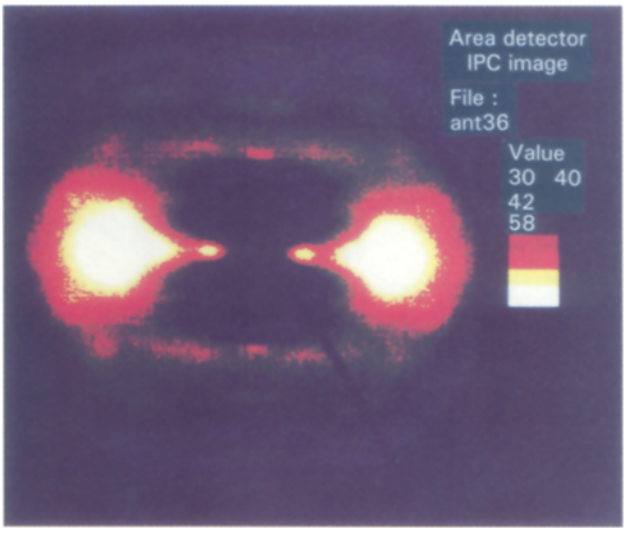

Figure 4 WAXS patterns (area detector) of as-spun and quenched PES fibres at room temperature. The X-ray wavelength is 0.154 nm, and the range shown corresponds to scattering angles of approximately − 35° to + 35 °C. Different colours indicate different intensity levels.

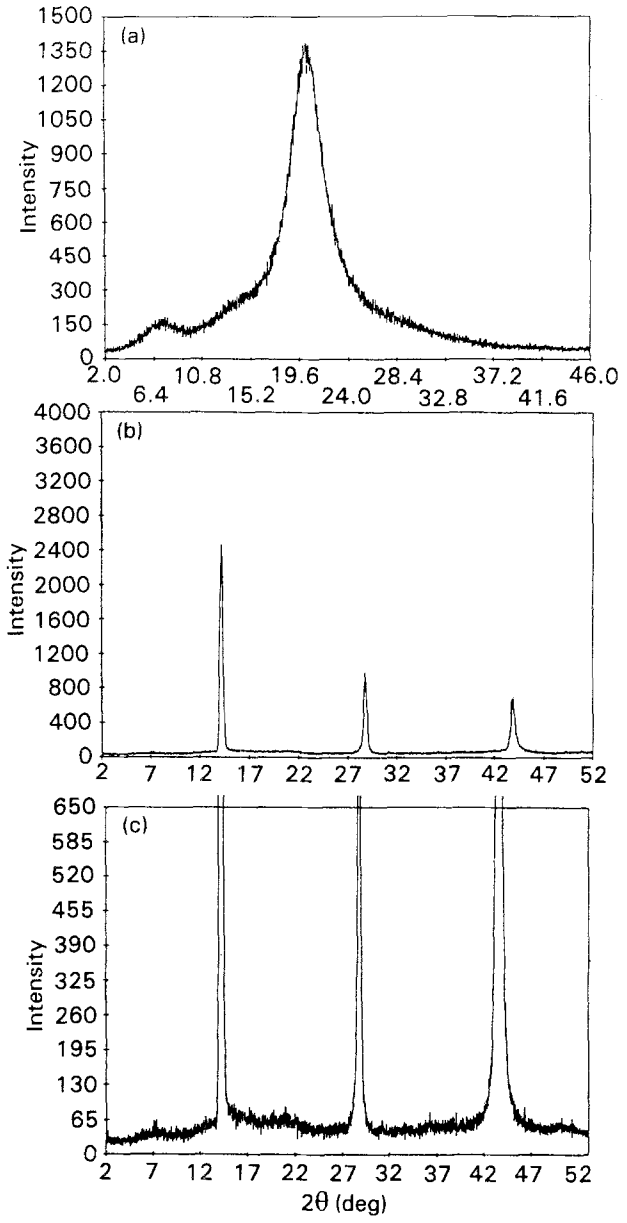

Figure 5 WAXS diffraction curves (θ–θ diffractometer) of as-spun and quenched PES fibres at room temperature: equator (a), meridian with normal (b) and strong (c) amplification.

the equatorial diffusive halo and the meridian intensity (Fig. 5) distributed both along the odd and even layers correspond to an oriented nematic phase, which is probably in the glassy state at room temperature. The X-ray pattern of this phase would be typical for scattering from an ensemble of single stiff macromolecules without correlation in the meridian direction between them, giving rise to reflections from the intramolecular order, while the equatorial halo corresponds to the liquid-like order of the chain centres in the plane perpendicular to the molecular axis.

As to the second phase, it is not difficult to suggest its nature. The existence of the long-range periodicity along the chain axis (sharp meridional reflections in the even layers) and weak but well-pronounced Bragg reflections at the equator and in the quadrants indicate a three-dimensional structure, namely a crystalline phase. Taking into account that the half-width of the meridional Bragg peaks is very small (0.3°), close to the experimental resolution, it is reasonable to assume an ordered arrangement along the macromolecular axis over the coherence length with long-range order larger than 100 nm. Since, on the other hand, equatorial peaks are much broader, the lateral crystallite sizes are much smaller and less than 10 nm. Thus, this crystalline phase may be identified as a polycrystalline structure, the crystals of which have anisotropic needle-like form.

Small lateral sizes of the crystallites are quite understandable if one takes into account that we are dealing with crystallization of random copolymers with different side groups during quenching. Well-ordered structures along the chain backbone are caused by the fact that all three comonomers have the same unit lengths of about 0.62–0.64 nm and the main chain can be expected to be very stiff.

On the basis of the proposed two-phase model the X-ray pattern of the quenched PES fibre can be satisfactorily described. One may expect, on the other hand, that the copolymer, in a similar way to other semi-crystalline polymers, should show a long spacing in the meridian direction in a small angle X-ray pattern. Fig. 6 shows SAXS data obtained for the quenched PES fibre. Only diffuse scattering is observed in the meridian direction, indicating the absence of a long spacing. This, however, does not mean that the assumption of the two-phase structure is wrong. It is well known that the appearance of discrete maxima in SAXS patterns is mainly due to the existence of alternating crystalline and amorphous regions, assuming that the difference of electron densities between the two phases is high enough. In our case the contrast between phases may be too small, as similarly observed for example for the flexible chain poly-4-methylpentene-1 [9]. This would explain why a long spacing peak is absent in the SAXS pattern.

Another explanation may be seen in the absence of a regular arrangement of phases. An amorphous phase in the usual sense would be difficult to understand anyway, because of the stiff nature of the backbone. A third possible explanation may be that the value of the long spacing is so high that the resolution of the small angle scattering setup (~50 nm) is insufficient. Indeed, it was mentioned above that the longitudinal crystallite size may be about 100 nm. Perhaps this is the most probable reason for an absence of the long spacing.

Small angle diffuse scattering is also observed in the equatorial direction of the SAXS pattern (Fig. 6), but with higher intensity than that in the meridian. The equatorial diffuse scattering is typical of a porous system (see, for example, [10]), indicating the existence of microvoids randomly distributed along the direction normal to the fibre axis (e.g. air between the fibres).

Fig. 7 shows equatorial diffraction scans obtained for fibres annealed at different temperatures, corresponding to the DSC scans previously shown in Fig. 3. The character of the X-ray patterns remains qualitatively the same for annealing temperatures up to 180 °C. At higher temperatures the peak intensities of the first two reflections increase, while the half-widths decrease. This behaviour is typical for a recrystallization process in the system. Besides, at least two more

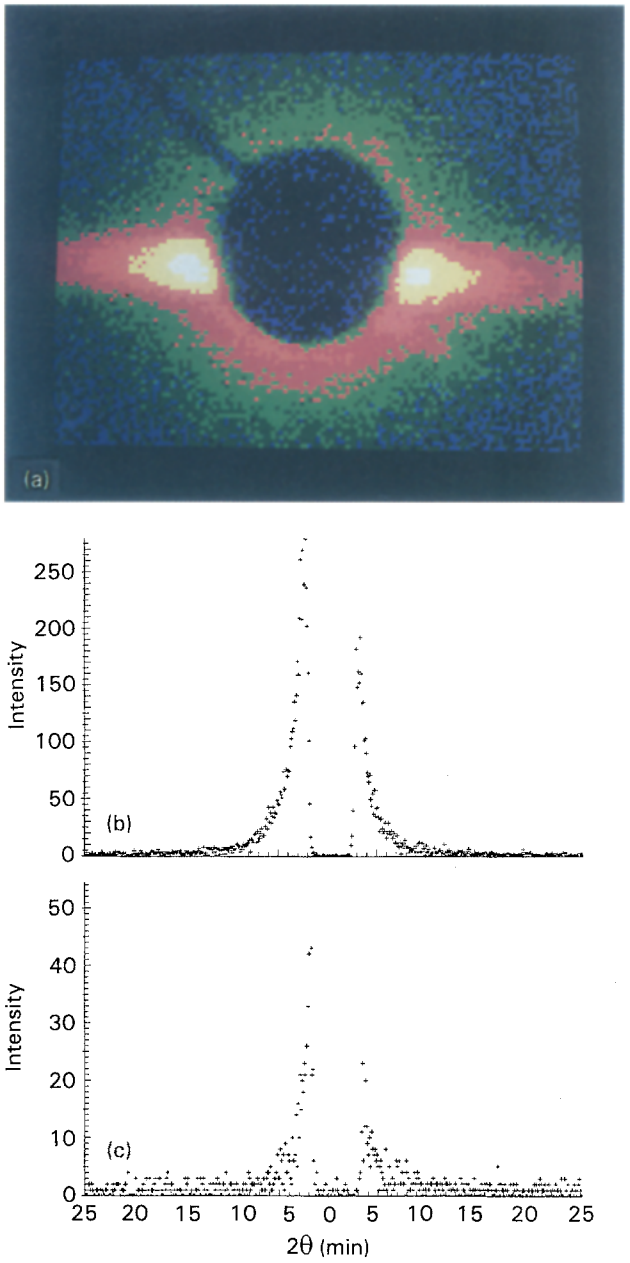

Figure 6 SAXS data (area detector) for the as-spun (quenched) PES fibre: 2D diffraction pattern (a), as well as equatorial (b) and meridional (c) scans through (a).

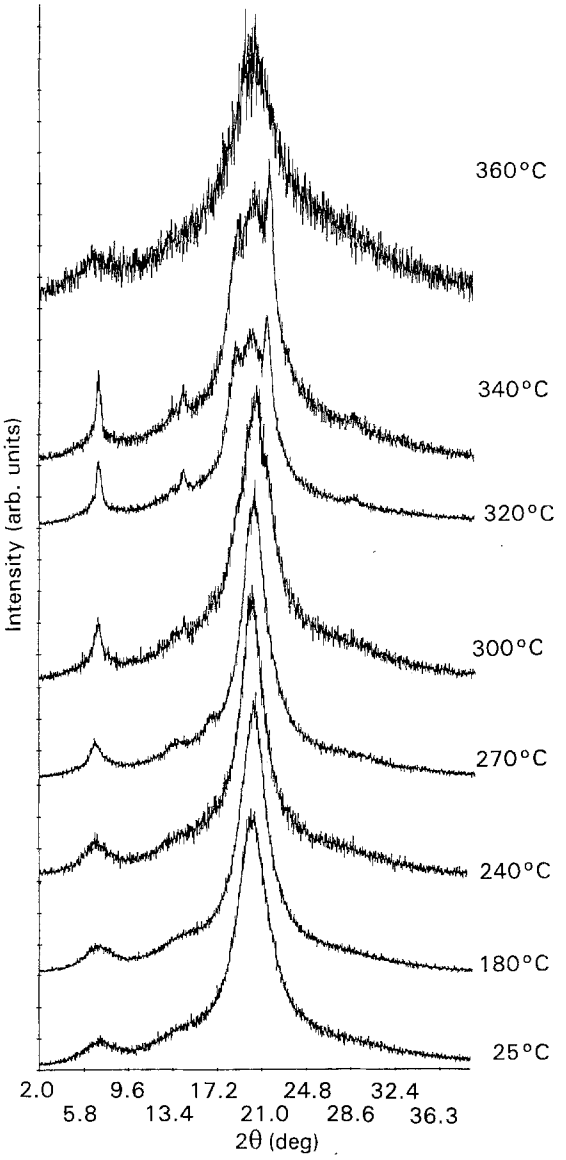

Figure 7 Equatorial diffraction curves (θ–θ diffractometer) of the PES fibres annealed for 4 h at the indicated temperatures (see also Fig. 3).

reflections at $2\theta \sim 16.5°$ and 29° at the equator and a set of reflections in the non-zero layers show up after annealing at 270 °C, indicating a well-developed three-dimensional crystalline structure (Fig. 8a). The formation of crystal lattice, which may be called crystal I, is completed at 270 °C. With a further increase of the temperature above 270 °C, melting of crystal I and the development of a new crystal modification takes place.

From the DSC traces (Fig. 3) one may suggest that melting of crystal I phase (the low temperature endo-effect in the DSC trace) is completed at 280 °C. On cooling of fibres previously heated to temperatures up to 280 °C or higher, the crystallization of crystal I is again observed (the low temperature exo-effect in the cooling trace) in Figs 1 or 2. This explains why the X-ray images obtained for fibres annealed at a temperature above the melting point of crystal I, followed by quenching, always comprises reflections of this crystalline phase.

The X-ray pattern of a PES fibre annealed at 300 °C or higher (Fig. 8b) shows well-pronounced Bragg reflections at the equator and in meridian direction, as well as in the quadrants, corresponding to a second crystalline modification which we call crystal II. The development of this phase is completed at ~ 340 °C. Its melting (the second endotherm in the DSC trace during heating in Fig. 3) begins above this temperature. Finally, annealing at 360 °C or higher temperature results in nearly the same X-ray patterns as obtained for the initial quenched fibre.

It should be noted that on rapid cooling of a sample previously heated above the melting point of form II, it also contains the first crystalline modification I. This is revealed by the well-pronounced low temperature exotherm (Fig. 1) observed during cooling, which has been attributed to crystal I formation, in contrast to the smeared high temperature endo-maximum in the DSC trace during cooling. Crystal II is believed to be the equilibrium structure (in contrast to crystal I), since it is exclusively formed during slow cooling or under prolonged annealing near to the melting point.

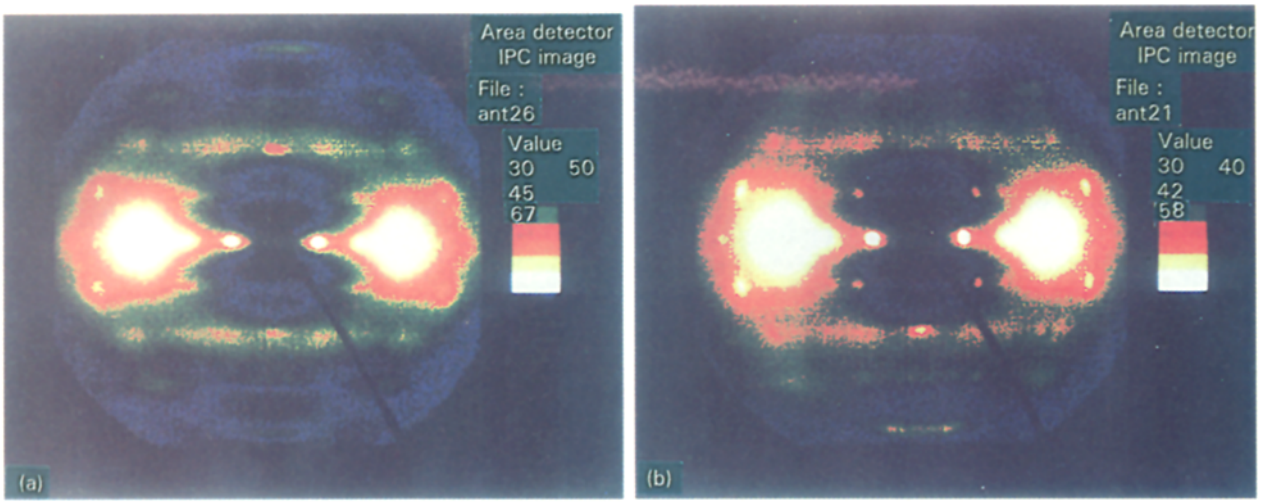

Figure 8 WAXS patterns (area detector) of PES fibres annealed at 270 °C (a) and 340 °C (b).

The existence of slow and fast crystallization processes with different structures has been found previously [4, 5] in a study of the crystallization kinetics of another thermotropic copolyester.

Thus, on the basis of the X-ray measurements it is possible to interpret the DSC data in the following way. The broad endotherm observed in the DSC heating trace of the as-spun sample (Fig. 9) in the temperature range 150–270 °C corresponds to a recrystallization process of the crystal I modification followed by melting of this crystalline form above 270 °C (the endotherm indicated by the lower dashed line in Fig. 9). Simultaneously, an exothermal process at ~ 280 °C (upper dashed line in Fig. 9) is beginning just above this temperature, corresponding to the crystallization of the crystal II modification. As mentioned above, the crystal II is the more stable phase as compared to crystal I and has, consequently, the higher melting point at 300 °C (the second endothermal peak in Fig. 9). The third endo-effect in the DSC trace indicates that between 300 and 320 °C still another structural form of the copolyester under investigation exists. This is neither a crystalline phase nor a LC nematic state, because, first, the reflections of the crystalline forms have disappeared above 300 °C in the X-ray pattern and, second, a LC nematic phase with long-range orientational order (the system is birefringent) is observed at still higher temperatures up to 360 °C, where finally the transition to the isotropic melt takes place. This phase between 300 and 320 °C might thus be called a "mesophase" and its detailed nature is presently still unclear.

With annealing of the PES fibres at higher temperatures, previously observed transition temperatures

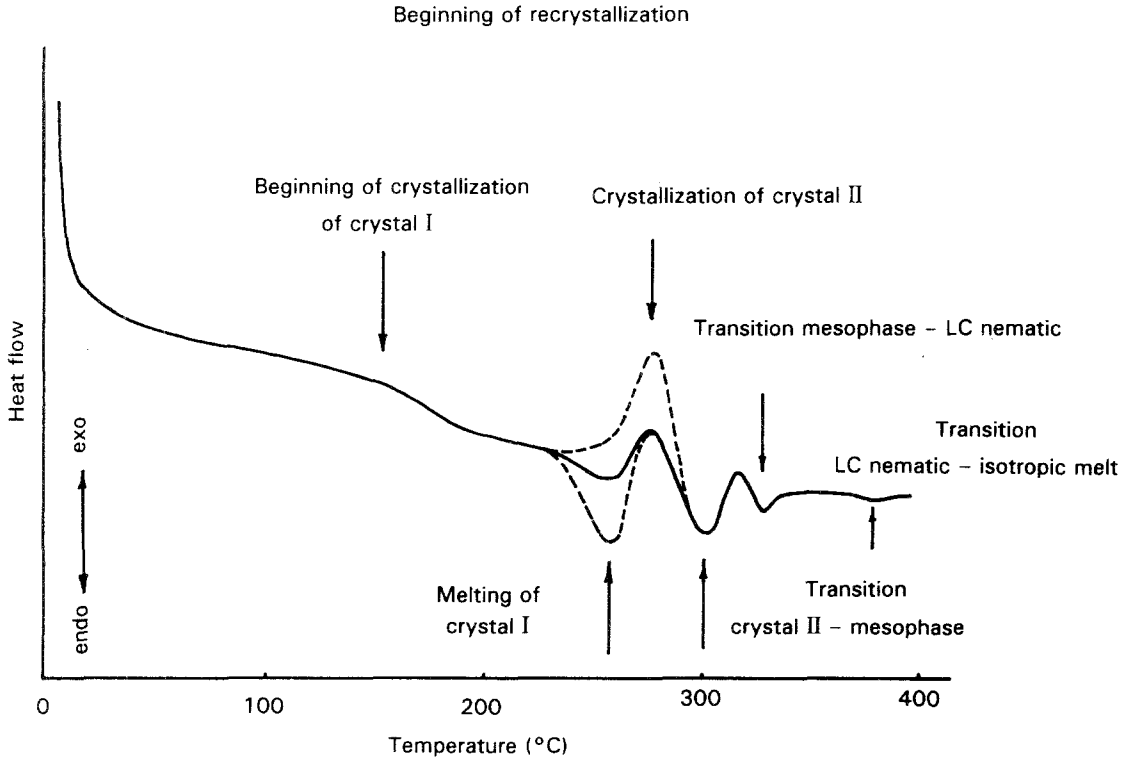

Figure 9 DSC trace during heating of the as-spun PES fibre including a schematic interpretation of observed features during heating.

are shifted or phases may be completely suppressed. When the annealing procedure is performed at temperatures below the melting point of crystalline form I (i.e. at $T < 270\,^{\circ}C$), the general behaviour of the DSC traces remains essentially the same. Low annealing temperatures only effect the low temperature "tail" of the recrystallization process, while the high temperature part of the curves is practically unchanged. After extensive annealing at 270 °C the recrystallization process of crystal modification I is almost suppressed in the DSC trace. At still higher annealing temperatures the endotherm corresponding to the melting of crystal I also disappears and the system crystallizes directly in the more stable crystal modification II. The melting endotherm of this modification is well defined in the DSC traces of the samples annealed at 300–340 °C (Fig. 3). An increase of the annealing temperature leads to an obvious shift of the endo-maximum towards higher temperatures. It can be explained by an increase in the size of modification II crystals and the equilibrium melting point of crystal lattice II is shifted to nearly 350 °C or even more. Finally, a heat treatment at 360 °C or above with subsequent quenching allows us to freeze the crystal II structure coexisting with the mesophase or LC state at room temperature.

Of course, this classification, in particular of the high-temperature transitions, is rather preliminary. The identification of high temperature mesomorphic structures is only possible rigorously as a result of X-ray analysis directly at those temperatures. This work is in progress and will be discussed in a future paper. Here we shall now concentrate on a better characterization of the crystalline modifications I and II.

3.2. Determination of crystal unit cells

The X-ray patterns of PES fibres annealed at 270 °C and 340 °C are shown in Fig. 8. To begin with we shall analyse the structure of the fibre annealed at the higher temperatures (300–340 °C), i.e. of the crystalline form II.

Annealing leads to the development of sharp Bragg reflections, pointing to an ordered three-dimensional structure for the copolymer investigated. Along the equator (Figs 8 and 10) there are at least five diffraction spots which can be identified. Along the meridian, periodic diffraction spots are observed up to the fourth layer line (Fig. 11). If the axis of the fibre is slightly tilted to the X-ray primary beam, even the sixth layer line will be visible. It is otherwise not in reflection condition. The even numbered layers show very low intensity, indicating that the crystal has a space group close to $P2_1$. In the quadrants (Figs 10 and 11) four diffraction spots along the first layer line, three (besides the meridional one) along the second and two along the third layer line can be precisely distinguished. Thus, a total of nineteen Bragg reflections (see Table I) are considered in the determination of the crystal unit cell.

As in the case of the quenched sample, the existence of the strong diffusive halo at the equator and the

TABLE I Characteristic data of meridional and equatorial reflections of crystal II modification at room temperature: assignment of Miller indices, scattering angle 2θ, d-spacing and intensity I

hkl	2θ (degrees)	d (nm)	I
100	7.49	1.228	very strong
200	14.44	0.639	strong
020	18.88	0.470	strong
300	21.64	0.410	very strong
400	29.36	0.305	medium
011	11.56	0.766	medium
201	14.53	0.610	medium
121	19.59	0.453	weak
031	26.74	0.333	strong
002	14.33	0.618	very strong
102	16.15	0.549	medium
022	22.75	0.391	very weak
302	25.19	0.354	weak
013	22.99	0.387	weak
123	27.83	0.321	very weak
223	33.75	0.266	weak
004	28.93	0.308	very strong
104	35.00	0.256	medium
006	44.06	0.205	strong

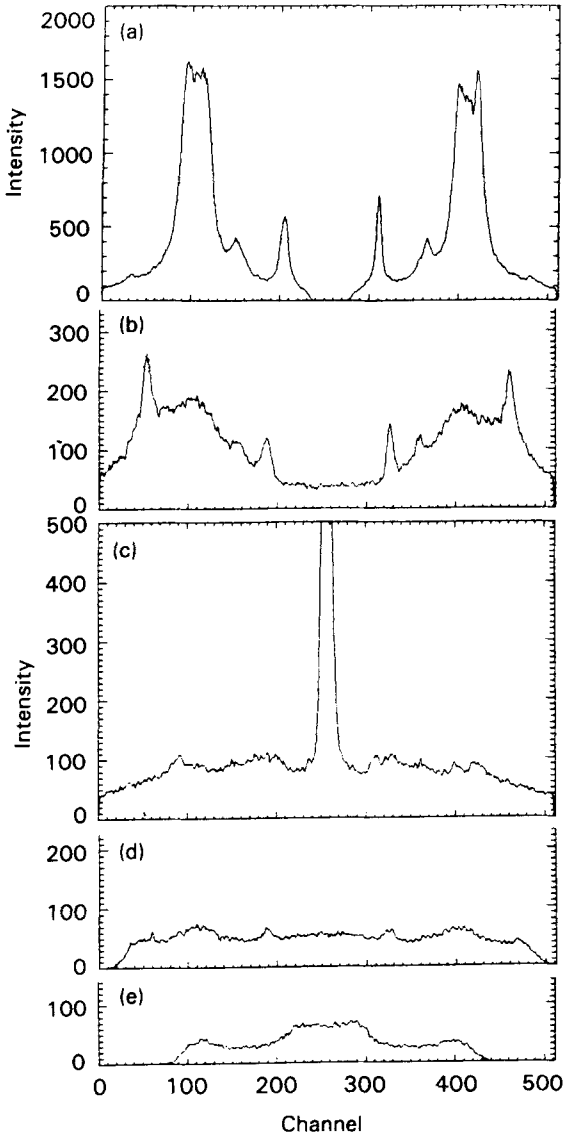

Figure 10 Scattering distribution (from a scan through the image of the area detector) along the 0th (a), 1st (b), 2nd (c), 3rd (d) and 4th (e) layer lines for the pattern shown in Fig. 8b.

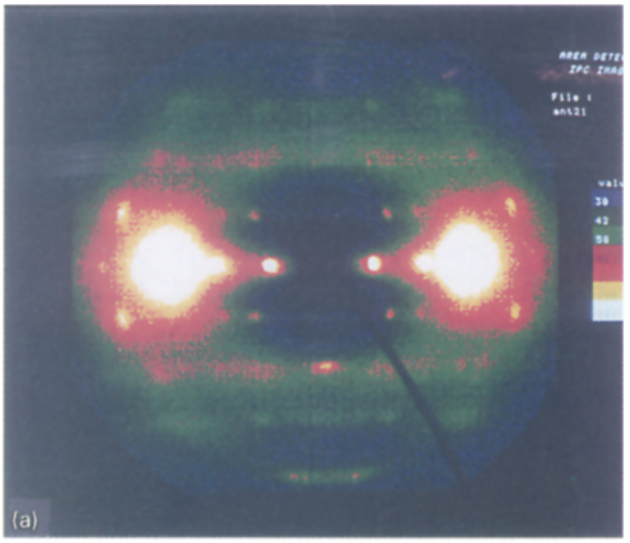

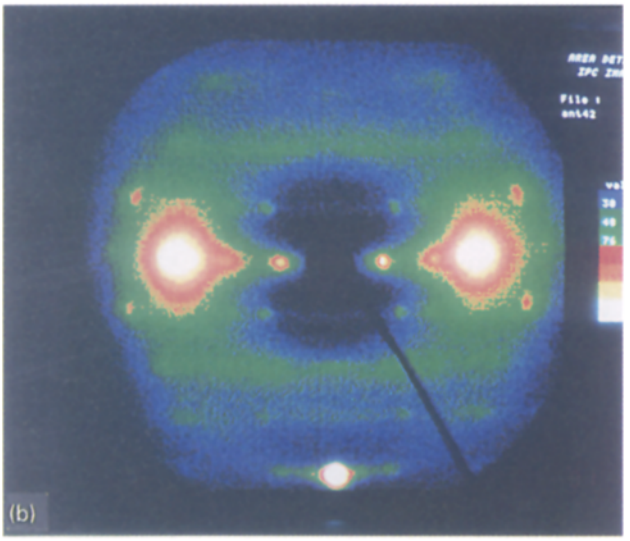

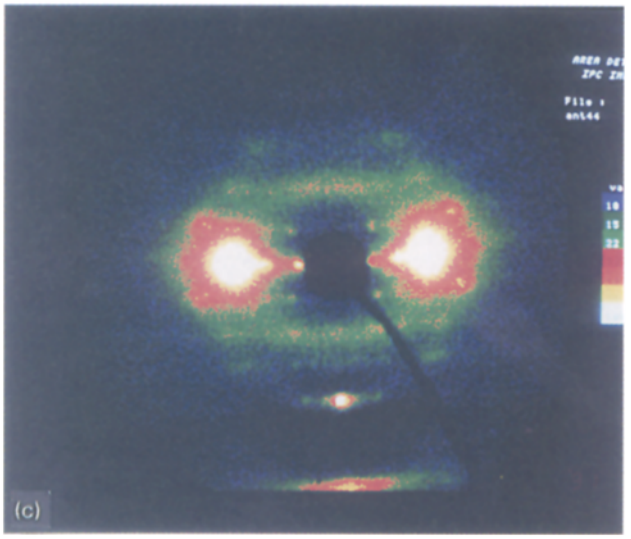

Figure 11 WAXS patterns (area detector) of the PES fibre annealed at 340 °C obtained with light (a), medium (b) and strong (c) tilts of the sample axis with respect to the primary beam. With increasing tilt, higher layer lines are in reflection condition and become visible on the area detector. The last image is taken at a smaller sample detector distance.

distribution of the weak intensity in even and odd layer lines leads to the suggestion of the coexistence of two phases for annealed PES fibres: crystal II and

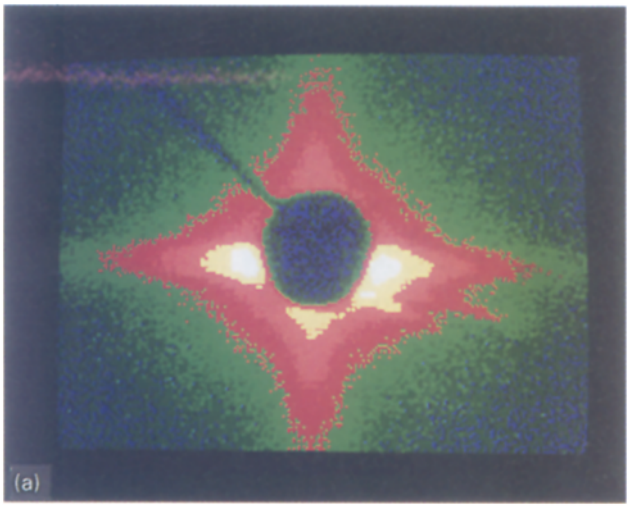

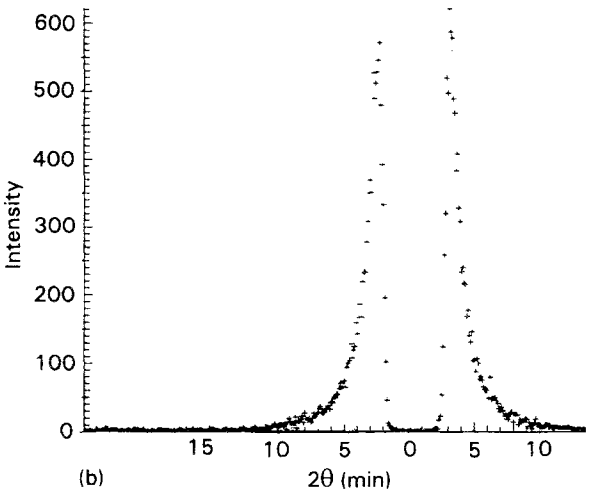

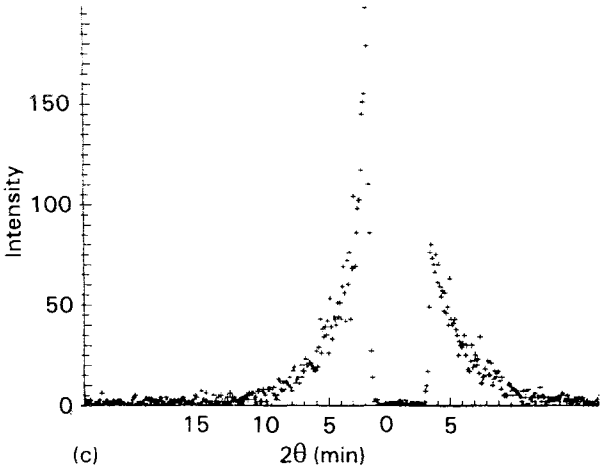

Figure 12 SAXS data (area detector) for the PES fibre annealed at 340 °C: 2D diffraction pattern (a), as well as equatorial (b) and meridional (c) scan through the pattern of (a).

frozen mesophase or LC nematic states. Again, a long-range periodicity is not observed in SAXS measurement. As shown in Fig. 12, there is no Bragg reflection resolved in the SAXS pattern. However, unlike the quenched sample, strong diffuse scattering is observed now not only along the equator but also along the meridian. The "cross"-like figure in the SAXS pattern of the annealed PES fibre again indicates the existence of microvoids in the system. It is now not a needle-like morphology, as was observed for the as-spun fibre (Fig. 6), but a square-like porous structure.

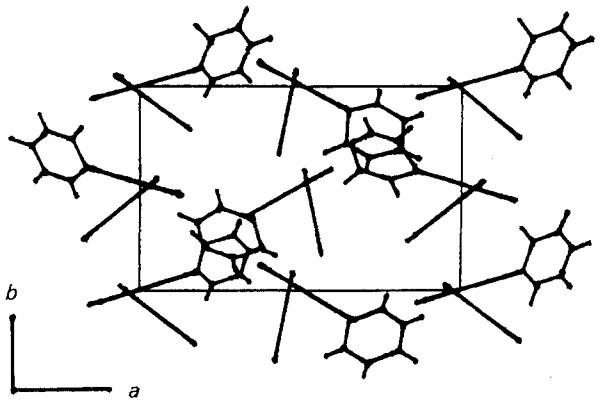

Figure 13 Orthorhombic unit cell of PES copolymer in crystal modification I: projection of four chains on the *ab* plane.

To determine the size and shape of the crystal unit cell from the fibre diagrams, we try to find an $hk0$ reciprocal lattice, namely a parallelogram with edges a^* by b^* which accounts for the peak positions determined from the equatorial diffractions. The smallest distance between the center of the primary beam and the diffraction spot corresponds to the lowest index. The l indices of diffraction spots can be determined from the corresponding layer lines on which the diffraction spots are located and the c crystallographic axis is readily determined from the layer line spacing, assuming an orthorhombic cell. So all diffraction spots shown in Fig. 8 can be identified as shown in Table I.

From a least-square refinement it is found that the crystal II unit cell of annealed PES fibre is orthorhombic with the following unit cell parameters: $a = 1.234$ nm; $b = 1.072$ nm; $c = 1.242$ nm. Each unit cell contains four chains (Fig. 13).

Following the same procedure, one can determine the unit cell parameters of crystalline form I, which is observed for the as-spun quenched fibre and for the samples annealed at temperatures equal to or below 270 °C. There are sixteen reflections in different layer lines which can be used for the fit. Assignments of peaks are given in Table II. In this case one also obtains an orthorhombic lattice, but with different unit cell parameters: $a = 1.315$ nm; $b = 1.072$ nm; $c = 1.242$ nm. Experimental angles and d-spacings for the observed reflections of crystal form I are listed in Table II. A summary of crystallographic data is presented in Table III.

TABLE II Characteristic data of meridional and equatorial reflections of crystal I modification at room temperature: assignment of Miller indices, scattering angle 2θ, d-spacing and intensity I

hhkl	2θ (degrees)	*d* (nm)	*I*
100	6.75	1.309	strong
200	13.34	0.663	medium
020	16.49	0.537	medium
300	20.31	0.437	strong
410	29.16	0.302	medium
011	11.84	0.747	weak
201	14.61	0.606	medium
121	20.25	0.439	weak
031	26.81	0.333	medium
002	14.25	0.621	very weak
102	16.15	0.549	weak
302	25.40	0.351	weak
003	22.00	0.404	medium
013	22.75	0.391	weak
004	28.70	0.311	strong
006	43.59	0.207	strong

TABLE III Crystallographic data for the two modifications of the pes copolyester under investigation

	Crystal I	Crystal II
a (nm)	1.315	1.234
b (nm)	1.072	0.942
c (nm)	1.242	1.225
Volume (nm^3)	1.750	1.424
Repeat units/unit cell	4	4
Space group	$P2_1$	$P2_1$

4. Conclusions

Detailed X-ray and DSC studies of the thermotropic main-chain liquid-crystalline PES copolyester under investigation reveal the existence of various phases observed in different temperature ranges. The material is highly oriented due to fibre processing, and X-ray fibre patterns show, up to 340 °C, sharp Bragg reflections. Two crystallographic modifications are identified with orthorhombic structure and slightly different unit cell parameters. While these "crystal I" and "crystal II" phases are observed up to 270 °C and 340 °C, respectively, under certain conditions indications are seen of a novel mesophase followed by a nematic liquid crystalline phase and the isotopic melt.

This phase sequence is, in particular, deduced from DSC heating and cooling scans, as well as from the observed modifications after annealing at different temperatures. The crystalline phases have been investigated by WAXS *in situ* and up to 19 Bragg reflections could be indexed and assigned to the orthorhombic unit cells. The high temperature phases were examined only after a quench to room temperature by X-ray scattering. A long spacing in SAXS is not observed in either case.

Thus the crystalline forms are well characterised, while one might only speculate — following for instance [1] — that the new phase between the high temperature "crystal II" structure and the nematic liquid crystalline state could be a condis mesophase of the PES copolymer, which is believed to be a very stiff molecule. Further X-ray investigations of the high temperature phases are in progress.

The present investigations thus indicate that thermotropic main-chain liquid-crystalline copolyesters are an interesting class of polymers showing a variety of different phases. Due to their excellent temperature stability, low viscosity in the melt combined with easy processability and good mechanical properties they might be potential candidates for high performance materials in future applications.

Acknowledgements

We acknowledge the technical help of M. Bach, Dr G. Urban and Dr U. Göschel during the X-ray experiments.

References

1. B. WUNDERLICH, M. MÜLLER, J. GREBOWICH and H. BAUER, *Adv. Polym. Sci.* **87** (1988) 1.
2. L.-S. LI, G. LIESER, R. ROSENAU-EICHIN and E. W. FISCHER, *Makromol. Chem. Rapid Commun.* **8** (1987) 158.
3. S.-K. HONG and J. BLACKWELL, *Polymer* **30** (1989) 225.
4. *Idem., ibid.* **30** (1989) 780.
5. S. Z. D. CHENG, A. ZHANG, R. L. JOHNSON, Z. WU and H. H. WU, *Macromolecules* **23** (1990) 1196.
6. S. Z. D. CHENG, Z. WU, A. ZHANG, R. L. JOHNSON and H. H. WU, *Polymer* **31** (1990) 1763.
7. E. Y. POLUSHKIN, E. M. ANTIPOV, V. G. KULICHIKHIN and N. A. PLATE, *Rep. USSR Acad. Sci.* **315** (1990) 1413.
8. B. W. UNDERLICH, "Macromolecular Physics", Vol. 2, Ch. 7 (Academic Press, New York, 1976).
9. N. N. KUZMIN, E. V. MATUKHINA, N. N. MAKAROVA, B. M. POLYCARPOV and E. M. ANTIPOV, *Makromol. Chem. Makromol. Symp.* **44** (1991) 155.
10. E. W. FISCHER, P. HERCHENRÖDER, R. ST. J. MANLEY and M. STAMM, *Macromolecules* **11** (1978) 213.

Received 25 March
and accepted 26 October 1992